

Article

Significant Fragmentation of Disposable Surgical Masks—Enormous Source for Problematic Micro/Nanoplastics Pollution in the Environment

Alen Erjavec *, Olivija Plohl , Lidija Fras Zemljič and Julija Volmajer Valh 

Institute of Engineering Materials and Design, Faculty of Mechanical Engineering, University of Maribor, Smetanova 17, SI-2000 Maribor, Slovenia

* Correspondence: alen.erjavec@um.si

Abstract: The pandemic of COVID-19 disease has brought many challenges in the field of personal protective equipment. The amount of disposable surgical masks (DSMs) consumed increased dramatically, and much of it was improperly disposed of, i.e., it entered the environment. For this reason, it is crucial to accurately analyze the waste and identify all the hazards it poses. Therefore, in the present work, a DSM was disassembled, and gravimetric analysis of representative DSM waste was performed, along with detailed infrared spectroscopy of the individual parts and in-depth analysis of the waste. Due to the potential water contamination by micro/nanoplastics and also by other harmful components of DSMs generated during the leaching and photodegradation process, the xenon test and toxicity characteristic leaching procedure were used to analyze and evaluate the leaching of micro/nanoplastics. Micro/nanoplastic particles were leached from all five components of the mask in an aqueous medium. Exposed to natural conditions, a DSM loses up to 30% of its mass in just 1 month, while micro/nanoplastic particles are formed by the process of photodegradation. Improperly treated DSMs pose a potential hazardous risk to the environment due to the release of micro/nanoparticles and chloride ion content.

Keywords: DSM; micro/nanoparticles; leaching; artificial weathering; environmental pollution



check for updates

Citation: Erjavec, A.; Plohl, O.; Zemljič Fras, L.; Valh Volmajer, J. Significant Fragmentation of Disposable Surgical Masks—Enormous Source for Problematic Micro/Nanoplastics Pollution in the Environment. *Sustainability* **2022**, *14*, 12625. <https://doi.org/10.3390/su141912625>

Academic Editor: Ning Yuan

Received: 12 July 2022

Accepted: 30 September 2022

Published: 4 October 2022

Publisher's Note: MDPI stays neutral with regard to jurisdictional claims in published maps and institutional affiliations.



Copyright: © 2022 by the authors. Licensee MDPI, Basel, Switzerland. This article is an open access article distributed under the terms and conditions of the Creative Commons Attribution (CC BY) license (<https://creativecommons.org/licenses/by/4.0/>).

1. Introduction

Since the discovery of Bakelite in 1907 until now, the plastic industry has undergone exceptional development and has had a great impact on our daily life [1]. According to Plastics Europe, global plastic production is increasing enormously year by year. For example, 367 million tonnes of plastic were produced in 2020. Plastics Europe estimates that at least half of all plastics produced have a short lifespan [2].

With the outbreak of COVID-19 and the announcement of a pandemic on 11 March 2020 by the World Health Organization (WHO), the global demand for medical personal protective equipment (PPE) has increased [3]. As Park and colleagues note in their analysis, global production of PPE, a short lifespan product, would need to increase by 40% during the pandemic to meet crisis demand [4]. Prevention of human-to-human transmission of the virus SARS-CoV-2 has led to the worldwide consumption of disposable surgical masks (DSMs). The WHO estimates that 89 million medical masks are needed each month to deal with COVID-19 [3]. As Czigan and Ronkay note in their article, surgical masks provide protection and an effective way to keep the virus from circulating because they reduce the number of droplets that an infected person spreads in their environment. Therefore and consequently, protective masks were one of the most sought-after products last year [5].

With the increase in production and consumption of surgical masks in the world, new challenges are being posed to the environment due to the world's largest issue now—microplastics and, even worse, nanoplastics. The declaration of an epidemic due to COVID-19 has triggered a different kind of emergency: single-use plastic is on the rise

again worldwide, and much of the non-recyclable PPE is consequently disposed of in the environment causing potential chemical contamination [6] and potential ecotoxicological consequences [7,8].

Generally, DSMs are classified as “FFP1” masks according to the EU standard EN149 and are also known by the code N95, as they can achieve 95% filtration of particles with a diameter of 0.3 μm . They are composed of five parts [9] that include ear loops, nose wire, and three layers of microfibers or nanofibers, which are hydrophobic, skin-friendly, and non-allergenic (Figure 1). The filter layers are usually produced using melt-blown electrospinning technology. All three layers can be made from a variety of synthetic polymeric materials such as polypropylene, polyurethane, polyacrylonitrile, polystyrene, polycarbonate, polyethylene, or polyester, depending on the customer’s preference [5,7]. However, as it is a plastic product, it is expected that after usage, in the form of waste, it will have further negative impact on the already polluted environment [5,9].

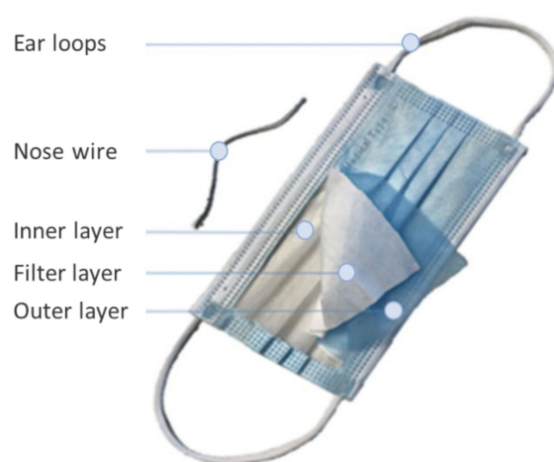


Figure 1. Composition of typical DSM with marked pieces.

Nowadays, DSMs are becoming a new and enormous source of plastic and micro/nanoplastics in the environment and causing severe pollution. For these reasons, it is of paramount importance to study the release of hazardous chemicals and fragmentation products from DSMs. A number of studies have already been published on the above topic, either containing only theoretical investigations on the negative effects of DSMs on the environment or focusing only on new DSMs from one or a few manufacturers. The studies mainly investigated the leaching of DSMs during the washing process or in artificial seawater [5–8,10–18]. In the context of aging experiments, Francesco Saliu and others [9] performed an initial and preliminary evaluation by subjecting commercially available surgical masks to artificial aging experiments, including UV irradiation and mechanical stress in artificial seawater. The results showed that a single surgical mask irradiated with UV light for 180 h and vigorously agitated in artificial seawater can release up to 173,000 fibers/day. Silvia Morgana et al. also state that a single mask in water can release thousands of microplastic fibers and up to 10^8 submicrometric particles, most of which are nanoscale [19].

The advantage of our study over other published studies is that we used a real sample—a mixture of used DSMs of different colors and from different manufacturers—to obtain a real representative sample. Our waste samples contained more than 30 different DSMs that are used daily in Slovenia. This is a much more heterogeneous sample than the ones used in similar studies where more homogeneous samples were used (usually less than 10 [8,16] or even only one type of DSM [6,17]). A representative sample consisting of DSMs was collected and a comprehensive study of the waste DSMs using a series of chemical, thermochemical, and physical analyses was conducted to characterize the DSMs as waste. Gravimetric analysis of larger samples (100 masks) and a complete waste characterization has been carried out in accordance with EU legislation.

In our study, special attention was paid to the potential water pollution from micro/nanoplastics generated by the degradation of these masks and also from other harmful components of DSMs generated during the leaching and photodegradation process, highlighting their adverse effects if not disposed of properly. For this purpose, two methods, a xenon arc fading lamp test in accordance with standard ISO 105-B04:1994 and toxicity leaching procedure (TCLP), were used, to analyze the production and characteristics of micro/nanoplastics [8,12,13,16].

In the xenon test chamber, the weathering resistance of the DSM was evaluated using different light spectra, temperatures, and humidity. In this way, the study of weathering and accelerated aging tests is made possible by closely mimicking actual environmental conditions.

2. Materials and Methods

2.1. Sampling and Gravimetric Analysis

The waste DSM sample was collected in a collection campaign in the faculty of the Mechanical Engineering University of Maribor. In the campaign were participating students, professors, and staff employed in the faculty who regularly delivered spent DSMs. During the campaign, over 10,000 spent DSMs were collected. A sampling of the whole collected sample was carried out according to a standard [20] to collect a representative sample for further analysis. Particular caution was given when collecting and sampling, due to the potential infectiveness of the material.

The surgical masks were divided into 5 basic components—nose wire, ear loops, outer non-woven layer, melt-blown filter layer, and inner non-woven layer—and was dried to constant mass. On a sample of 100 disassembled masks, we performed a gravimetric analysis of the proportion of each component in our sample. The masks were disassembled manually. Each component was weighed on a Kern ALT 220-4NM balance with an accuracy of ± 0.001 g.

2.2. Characterization of Physicochemical Properties of Surgical Masks

The DSMs were analyzed with the spectrometer ATR FTIR Perkin Elmer Spectrum GX (Perkin Elmer FTIR, Omega, Ljubljana, Slovenia). The ATR accessory (supplied by Specac Ltd., Orpington, Kent, UK) contained a diamond crystal. A total of 16 scans were taken of each sample with a resolution of 4 cm^{-1} . All spectra were recorded at ambient temperature over a wavenumber interval between 4000 and 650 cm^{-1} . Four measurements were performed for all 5 parts and on both sides of each layer of DSMs. Pristine DSMs were also characterized in terms of thermogravimetric properties and DSC as explained below.

2.3. Waste Characterization

In accordance with the Slovenian regulation [21] that is modeled after Council Directive 1999/31/EC, chemical thermogravimetric and additional physicochemical analyses were performed to carry out the characterization of waste. First, a sample was prepared in accordance with the standard [22]. The metal wires were removed from the sample and the remainder was ground into fine dust using an A 10 IKA Werke mill with a water-cooling system. Fifty grams of milled sample was produced which is roughly equal to the mass of 100 masks. So, it contained all 3 layers of the mask, ear loops, type 3 nose wire, and type 1 and 2 plastic coating of the nose wire (in accordance with Figure 2). With the obtained sample, the determination of the content of metal elements was carried out using inductively coupled plasma with optical emission spectrometry (ICP-OES) in line with the standard [23]. As in the standard [24], the determination of total organic carbon (TOC) in waste was performed. The nitrogen content was determined according to the standard [25] and hydrogen using the Dumas method [26]. Similar to the standard [27], the determination of loss on ignition was carried out and the dry matter content according to the standard [28] method A. Determination of gross calorific value and calculation of net calorific value were also carried out as in the standard [29]. Other methods that have been used were the

determination of polychlorinated biphenyls (PCBs) [30] and the determination of chlorine (Cl), fluorine (F), and sulfur (S) [31].

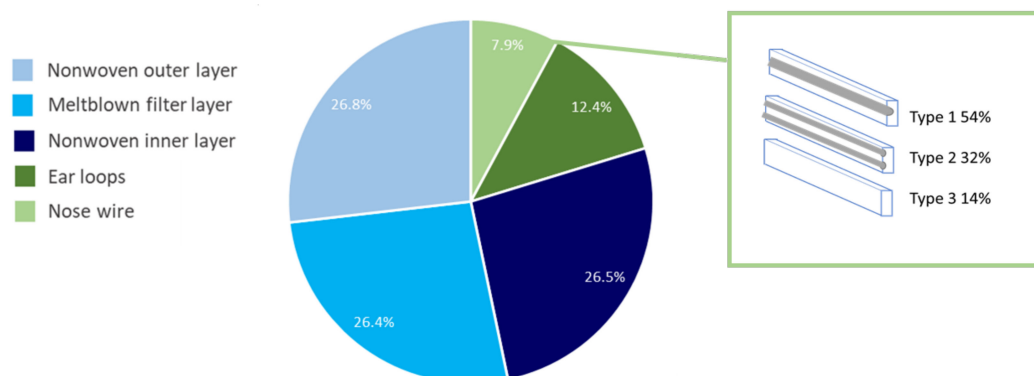


Figure 2. Gravimetric analysis of various DSM compositions shown as a percentage with included types of nose wire and their proportion in our sample.

2.4. Toxicity Characteristic Leaching Procedure (TCLP) and Analysis of TCLP Products

The toxicity characteristic leaching procedure (TCLP)—SW-846 Test Method 1311 [32]—was performed to determine the mobility of both organic and inorganic analytes present in samples. A representative sample of DSMs was prepared in the following way: all 5 parts (nose wire, ear loops and outer, filter, and inner layer) were cut into pieces smaller than 1 cm². Then, the dry matter of the sample was determined according to the standard [28]. The TCLP was performed for the whole mask and all 5 parts of the DSM separately. Six different samples were analyzed, and each was prepared in two parallels—outer layer, filter layer, inner layer, ear loops, nose wire separately and all parts together in mass proportions the same as for mask composition. This value was used in Equation (1) to determine the amount of distilled water that is needed to perform a TCLP of 50 g of our sample. Fifty grams of the sample was put in a glass jar with the correct amount of distilled water. Then, the jars were put on an HS-501 shaker made by IKA Werke that rotated at 30 ± 2 rpm for 18 ± 2 h.

$$m_{fluid} = \frac{20 \cdot w_{dry\ matter} \cdot m_{sample}}{100} \quad (1)$$

Products were first filtered through a colander with a mesh having a diameter of 5 mm, to remove larger parts. Then, obtained filtrate was filtered again through polyether sulfone (PESU) filters with an effective pore size of 0.2 µm and diameter of 50 mm, from Sartorius Stedim Biotech GmbH. Microplastics retained on the filter were examined under a Zeiss Axio Vision optical microscope with which different parts were observed and measured. Dried microplastics on the filter were also weighed and analyzed using an ATR FTIR Perkin Elmer Spectrum GX spectrometer as is described in Section 2.2. Filters used were dried to constant mass at 100 °C in a VS50-SC dryer produced by Kambič d.o.o. and weighed before the filtration. After filtration, they were dried again and weighed to determine the mass of microplastics on the filter. Filters were weighed on a Kern ALT 220-4NM balance with an accuracy of ±0.001 g. Obtained microplastic particles were also analyzed and measured under the optical microscope ZEISS Axiotech 25HD (+ pole), with an AxioCam MRC (D) high-resolution digital camera, and a Carl Zeiss FE-SEM SUPRA 35 VP scanning electron microscope with a GEMINI field emission module.

Water obtained in the TCLP before and after the filtration process was tested for simple qualitative properties. With a Velp Scientifica TB1 turbidimeter, turbidity of samples was measured and, with a Metler-Toledo SevenCompact S230 conductometer, conductivity of samples was measured. Chemical oxygen demand (COD) was also determined by using tube tests by Macherey-Nagel, Macherey-Nagel Nanocolor Vario 4 heating unit, and Macherey-Nagel Nanocolor UV/Vis spectrophotometer.

Water after filtration was also analyzed for particle size distribution (PSD) using a Zetasizer Nano ZS[®] (Malvern Instruments, Ltd., UK) equipped with dynamic light scattering (DLS) technology. Triplicate measurements were carried out using a He-Ne laser at a wavelength of 633 nm and scattering angle of 173° at 25 °C for 70 s.

2.5. Photodegradability of Mask

Photodegradation of the mask was performed by artificial weathering using a Xenotest alpha LM high-energy climate chamber (Atlas Material Testing Technology GmbH, 1500 Bishop Ct, Mount Prospect, Illinois, 60056, United States). It was essentially the same as the standard ISO 4892-2 2013, with minor modifications in cycle composition. The DSMs were manually prepared to fit into the Xenotest holders. The samples were then dried at 90 °C for 1 h to maintain a constant mass. The samples were then weighed and placed in the Xenotest. One cycle consisted of a 1 min rain period and a 29 min dry period at a relative humidity of 50% and a constant temperature of 38 °C. Irradiance was set to 60 W/m² and was provided with the use of a daylight filter. These laboratory conditions are a rapid simulation of the real natural conditions to which DSMs are exposed in nature, thus mimicking real conditions. A cycle was repeated 25 times, 50 times, 75 times, 100 times, 125 times, 150 times, 175 times, and 200 times. Samples were then dried again at 90 °C for 1 h and weighed. In addition to gravimetric analysis, we also performed FTIR analysis as well as thermogravimetric analysis (TGA) and differential scanning calorimetry (DSC) of the masks after aging. Distilled water was used for the simulated rainwater, which was collected and analyzed after the simulation. A few drops of the simulated rainwater were examined under a ZEISS Axiotech 25HD (+ pole) optical microscope. It was also filtered through a PESU filter with < 0.2 µm mesh size. The filtrate was analyzed by DLS to detect any nanoscale particles released from the samples.

TGA and DSC analyses of raw DSMs were also performed to assess possible changes. For TGA before and after Xenotest, a METTLER TOLEDO TGA 2 STAR System was used under air atmosphere in the temperature range 25–700 °C and with a heating rate of 10 K min⁻¹. For DSC, a METTLER TOLEDO DSC 3 STAR System was used under nitrogen (N₂) atmosphere in the temperature range of 25–700 °C and with a heating rate of 10 K min⁻¹.

3. Results

3.1. DSM Characterizations

3.1.1. Gravimetric Analysis

After manually decomposing 100 different DSMs into five components (shown in Figure 1), we used the basic statistical tools in Microsoft Excel to obtain the results shown in Figure 2. The average mass of a single mask was 3.1205 g. The maximum mass fraction of the mask represents a three-layered part, resulting in 79.7%. This percentage is evenly distributed among all three layers and most likely contributes to micro/nanoplastic fragmentation. Ear loops represent 12.4% of the mass of the DSMs, and the lowest percentage of the DSM mass is represented by nose wire, i.e., 7.9%.

In the obtained sample, three different types of nose wire were found. The most common one is nose wire composed of one metal wire coated with plastic (type 1) and is represented in more than half of all masks analyzed, the second one is composed of two metal wires coated with plastic (type 2), and the third one, the least represented type, is without metal wire, just plastic with additives that provide similar properties to metal wire in plastic (type 3). Schematic representations of all three types of nose wire are shown in Figure 2.

3.1.2. ATR-FTIR Characterization of Pristine DSMs

Similar to above, 50 different DSMs were manually decomposed into all five parts as shown in Figure 1 and analyzed by ATR FTIR spectroscopy. The results show the different spectra that were collected from each part. As can be seen in Figure 3a, two

different types of spectra of the non-woven outer layer and non-woven inner layer have been found. All collected spectra of the filter layer were the same. The spectra of one type of non-woven outer layer, filter layer, and one type of non-woven inner layer showed the following bands: multiple peaks in the wavenumber range from 3000 to 2800 cm^{-1} and two large peaks in the range from 1456 to 1375 cm^{-1} . The peaks in the range from 3000 to 2800 cm^{-1} were attributable to asymmetric and symmetric stretching vibrations of CH_2 groups, while the peaks at 2950 and 2850 cm^{-1} were due to the asymmetric and symmetric stretching vibrations of CH_3 . The peak at 1456 cm^{-1} indicates the asymmetric CH_3 vibrations or CH_2 scissor vibrations, while the peak at 1375 cm^{-1} was the result of the symmetric CH_3 deformation [33]. All mentioned signals represent typical signals for polypropylene materials.

The other two spectra, corresponding to the second type of non-woven outer layer and the second type of non-woven inner layer, presented only two signals in the range from 3000 to 2800 cm^{-1} , namely, at the wavenumber 2914 and 2848 cm^{-1} , signal at 1471 cm^{-1} , and the small peak at 717 cm^{-1} , that are identified as characteristic bands for C-H wagging vibrations (Figure 3a). Those signals are attributed to polyethylene materials [34]. Interestingly, among the 50 DSMs measured, only one was found to have a non-woven outer layer and a non-woven inner layer of polyethylene materials.

As can be seen in Figure 3b, four different spectra of ear loops with different positions of signals were obtained. Comparing the collected spectra with the spectra of synthetically produced untreated polyamide 6 [35], it was revealed that the characteristic peaks overlap. Typical bands that were found were assigned to polyamide 6, also known as nylon 6. However, slight variations between the spectra can be observed due to different manufacturers of ear loops adding different additives to provide desired properties of the product.

In the case of nose wire examination, the metal wires were removed first, and then only the plastic coating was analyzed. As already schematically shown in Figure 2, three different types of nose wires were found according to their structure. As they differ in structure, they also differ in the FTIR spectra obtained. Type 1 was a nose wire with a metal wire in a plastic coating. As can be seen in Figure 3c, the spectra of type 1 have peaks typical for polypropylene, and the position of bands is very similar to the spectra of the coatings of polypropylene in Figure 3a. Type 2 and type 3 nose wires' spectra are very similar, and they are compared with the spectra in Figure 3a, as they are also comparable to the inner and outer layer of DSMs made of polyethylene. Indeed, among all nose wires examined, the material polypropylene predominates.

3.2. DSM Characterization as a Waste

To better understand the potential risks posed by discarded DSMs, the total analysis was performed for DSMs in the form of waste by several standards (for details, refer to Section 2.3) to identify the possible release of chemical compounds when a mask is decomposing in the environment, that according to our knowledge has not yet been carried out, but has already been recommended [18]. In accordance with Slovenian regulation [21], the presence of trace elements was analyzed. The results of the detected items are shown in Table 1. All results are in milligrams from a kilogram of dry matter. Results of other analytical methods that were carried out are shown in Table 2.

The elemental analysis that was carried out showed that 73.99% of a waste DSM without metal wires is composed of total carbon (TC), 16.43% of nitrogen (N), and 6.95% of hydrogen (H). In the same sample, 0.63% chlorine (Cl) was also detected (Table 2) which is of particular concern. It should be noted that all results are calculated on dry matter. One of the possibilities is that chlorine gets into the masks during the sterilization process. As Van Loon and colleagues note, two processes that contain chlorine-containing chemical compounds also appear in the review of possible DSM sterilization processes. These are sterilization with bleach (sodium hypochlorite solution) and chlorine dioxide gas (ClO_2). The latter process is much more commonly used in practice and is very likely the reason for the presence of Cl in waste DSMs.

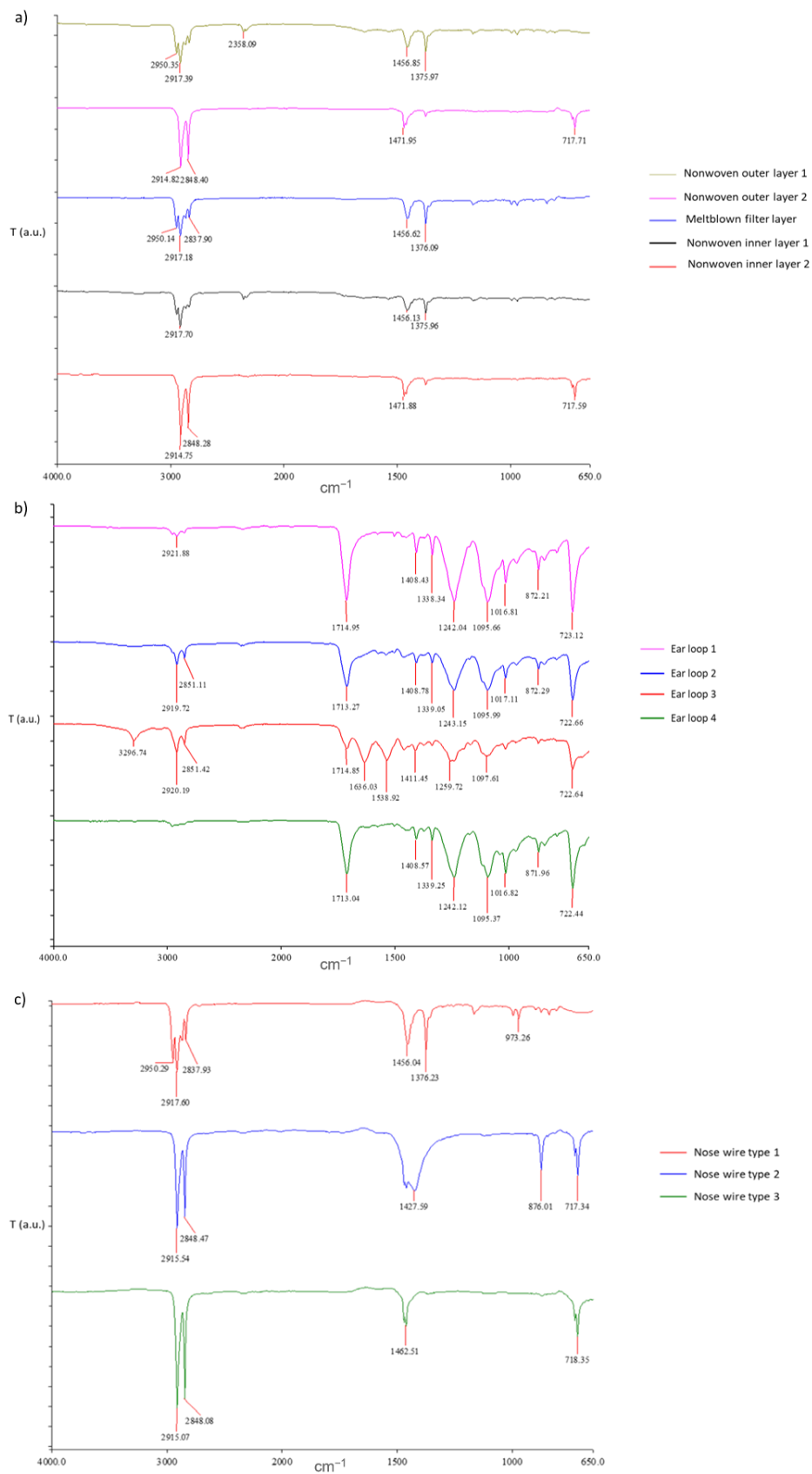


Figure 3. (a) FTIR spectra of 3-layered part of DSM; (b) FTIR spectra of different ear loops; (c) FTIR spectra of nose wires.

Table 1. Analyzed trace elements in waste DSM without metal wire.

Trace Elements	Value (mg/kg d.m.)	Trace Elements	Value (mg/kg d.m.)
Ag	<10	In	<10
Al	39.35	Li	<10
As	<3	Mg	78.41
Ba	<7	Mn	<8
Bi	<10	Na	50.04
Cd	<3	Ni	7.65
Co	<7	Pb	<5
Cr	13.09	Se	<3
Cu	15.42	Sr	<10
Ga	<10	Ti	<10
Hg	<1	Zn	51.97

Table 2. Other analyses to determine waste characterization.

Other Analysis	Value
Dry matter	>99%
Loss on ignition	>99%
Net calorific value	44,264 kJ/kg
Gross calorific value	45,739 kJ/kg
PCB	Not detected
Cl	0.63% d.m.
F	<0.2 mg/kg
S	<0.2 mg/kg

Based on the analysis of the metal content (Table 1), we can conclude that there is no detectable increased presence of metals in our sample. We should keep in mind that we removed the metal wires from the nose wire and analyzed only the polymer coating in the DSM mix sample. Since we provided analyses in accordance with the assessment of hazardous waste prior to incineration [21], there are no limit values. Yet, DSMs are expected to release elements (Table 1) when discarded that can contribute to the release of potentially hazardous chemicals such as Cr, with possible adverse ecological effects on wildlife, as already pointed out [7,15].

As is seen in the data in Table 2, this is a type of waste that is eminently suitable for energy use, as it has an extremely high dry matter content, while at the same time we can conclude from the loss on ignition that no significant amount of ash (less than 1%) is produced during combustion. The net calorific value is also extremely high, even exceeding the net calorific value of crude oil (42,300 kJ/kg) and being comparable to gasoline (\approx 44,300 kJ/kg) [36].

3.3. Toxicity Characteristic Leaching Procedure (TCLP) and Analysis of TCLP Products and Microplastic That Is Being Produced

Qualitative properties of the water and mass of isolated microplastics obtained in the TCLP are reported in Table 3. During the leaching process, most of the microplastic is released from the ear loops, followed by the inner layer, the outer layer, the filter layer, and the wire, in that order. This is reflected not only in the mass of microplastics larger than 0.2 μ m left on the filter but also in the highest COD, turbidity, and conductivity of the washout fluid. These findings were also confirmed by gravimetric analysis of

microplastic parts loaded on filters. The greatest mass of microplastic parts is released out of ear loops (28.9 mg) which is 0.23% of the original mass needed for the TCLP procedure. Table 3 shows that the turbidity of each DSM part decreased after filtration. A similar trend is also observed for COD, being smaller after TCLP filtration in all cases. Similarly, conductivity is lower or does not change after filtration. The release of microplastics on PESU filters increased after the TCLP in all parts of the DSM. It can be concluded that turbidity, COD, and conductivity values decrease due to removal of microplastics with the filtration process and that the presence of microplastics increases the values of these three water quality parameters.

Table 3. Simple qualitative properties of the water obtained in TCLP before and after filtration.

DSM Part	Before Filtration			After Filtration			$m_{\text{microplastics}>0.2 \mu\text{m}}$ (mg) Released on Filters
	Turbidity (NTU)	Conductivity ($\mu\text{S}/\text{cm}$)	COD (mg/L O ₂)	Turbidity (NTU)	Conductivity ($\mu\text{S}/\text{cm}$)	COD (mg/L O ₂)	
Blank	0.3	0.1	5.1	0.1	0.1	2.2	0
Outer layer	19.1	90.8	52.5	1.7	89.2	40.5	9.1
Filter layer	9.5	117.2	41.1	0.3	55.5	27.2	5.5
Inner layer	24.9	123.7	151.2	3.8	124.4	124.5	12.6
Ear loops	44.9	204.6	162.4	3.7	199.4	158.0	28.9
Nose wire	6.6	21.7	13.2	0.2	22.5	10.3	2
Whole mask	15.5	103.4	68.3	1.9	111.2	59.3	7.4

The microplastics that were being produced and were loaded on a PESU filter with an effective pore size of 0.2 μm were examined under the optical microscope and with ATR-FTIR analysis. Results of ATR-FTIR analyses of leached microplastic particles by every part of DSM are shown in Figure 4. Pictures made with an optical microscope are shown in Figure 5.

The FTIR spectra of the microplastic produced during the TCLP differ from the FTIR spectra of the base parts of the surgical masks (refer to Figure 3). The FTIR spectra of microplastic release from the outer, inner, and filter layers (Figure 4a–c) and also from the nose wire (Figure 4e) are not consistent with the spectrum of polypropylene, showing new peaks around 3300 cm^{-1} , 1650 cm^{-1} and peaks in the range of 1030–1060 cm^{-1} . The peaks in the range from 3000 to 2800 cm^{-1} , which are due to asymmetric and symmetric stretching vibrations of the CH₂ and CH₃ groups of polypropylenes, are less pronounced and the peaks at 1456 and 1376 cm^{-1} disappear completely in the spectra of the released microplastic. From this, we can conclude that polypropylene undergoes oxidation/degradation reactions that were confirmed with the appearance of new bands after the TCLP [16,18]. The new peak around 3300 cm^{-1} may correspond to hydroxyl groups, while the peaks in the range of 1030–1060 cm^{-1} may represent signals for C–O stretching vibrations [16]. The FTIR spectrum of microplastic released from ear loops (Figure 4d) differs from the polyamide 6 spectrum in the following two peaks: peak at 3295 and peak at 1635 cm^{-1} . The latter may also be attributed to the oxidation process of polymeric material [16,18].

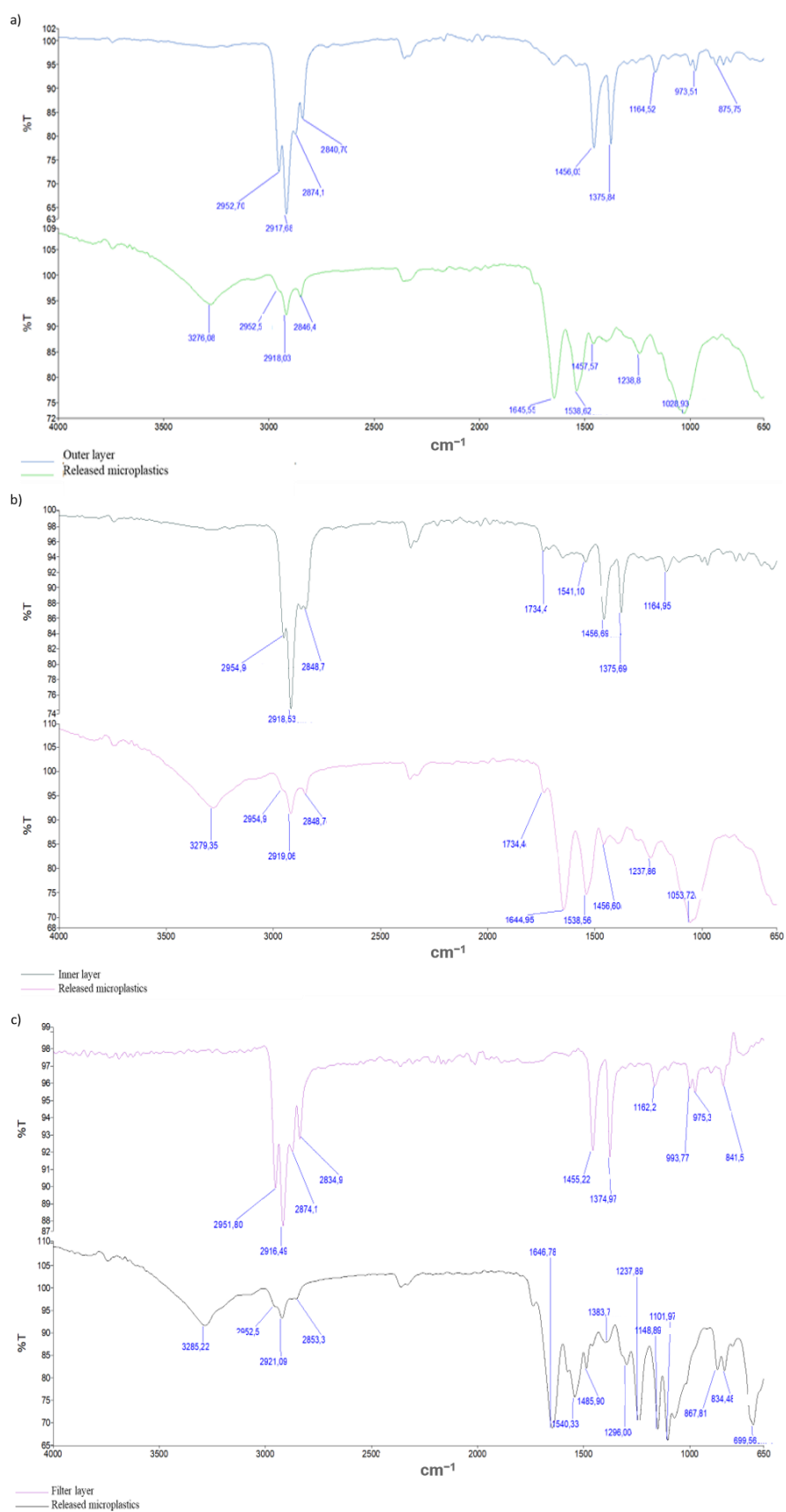


Figure 4. Cont.

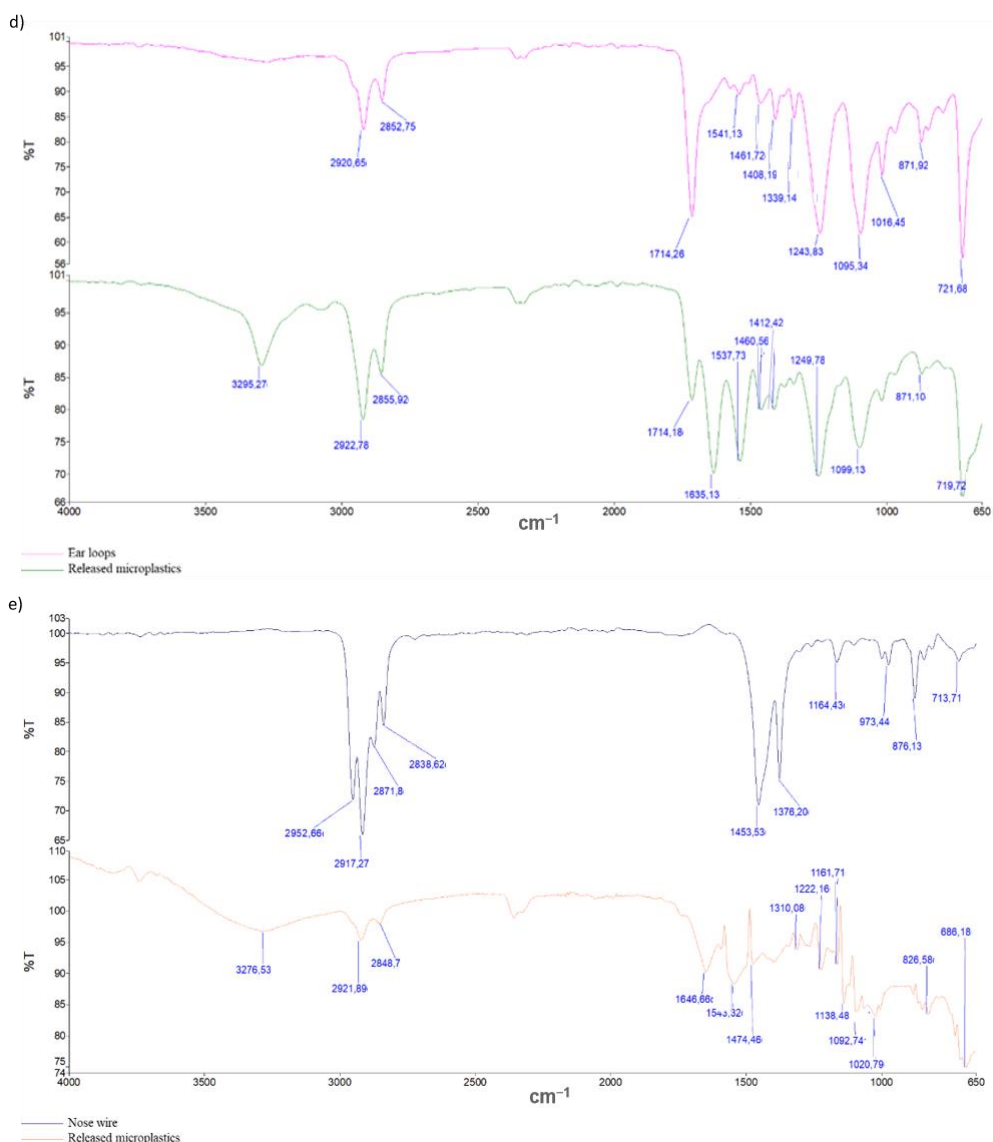


Figure 4. ATR FTIR scans of leached microplastic parts loaded on PESU filter with an effective pore size of $0.2\ \mu\text{m}$ with referential scans of each part before TCLP: (a) microplastic parts out of the outer layer, (b) microplastic parts out of the inner layer, (c) microplastic parts out of filter layer (d) microplastic parts out of ear loops, and (e) microplastic parts out of nose wire.

The microplastic particles in Figure 5b,d,f,h are quite similar. Most of the particles are fibers that are uniformly distributed and not superimposed. Some fibers are fragmented into particles and broken, which look like irregular spheres and cubes and are no longer fiber-like, as initial layers. Such morphology and shape of fiber-forming particles are expected because of the material from which they are leached (Figure 5a,c,e,g). In Figure 5j, the leached microparticles are different from those in the previous photographs. In this case, the particles are dislodged from nose wires (Figure 5i) and are made of hard polypropylene. The slightly orange color is probably the result of the presence of metal wire. It was shown in [15] that when other particle shapes and morphologies were compared to fiber-shaped particles, it was revealed that the latter in general tends to cause larger ecotoxicological effects.

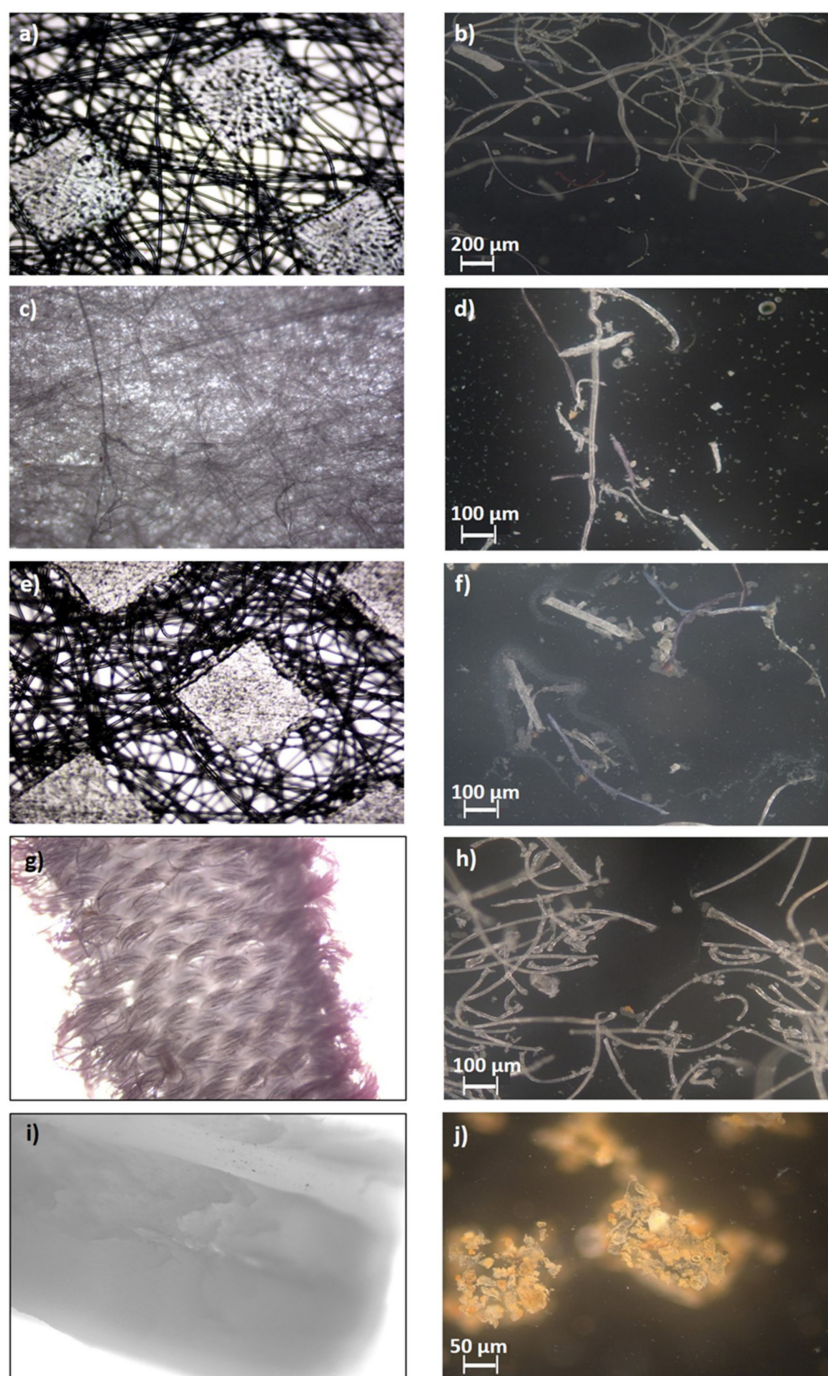


Figure 5. Optical microscope scans of pristine DSM parts before TCLP (magnified 4 times) and leached microplastic parts loaded on filters after TCLP (magnified 100 times): (a) pristine outer layer, (b) microplastic parts out of the outer layer, (c) pristine filter layer, (d) microplastic parts out of the filter layer, (e) pristine inner layer, (f) microplastic parts out of inner layer, (g) pristine ear loops, (h) microplastic parts out of ear loops, (i) pristine nose wire, (j) microplastic parts out of nose wire.

The TCLP products of the whole DSM sample were also analyzed by SEM (Figure 6a,b). Figure 6a show particles present in the analyzed leachate before filtration, and in Figure 6b they can be seen after filtration through filters with a mesh size of 0.2 μm . Accordingly, it is to be expected that in the first photo much larger particles can be seen, most of which are fibers that are uniformly distributed and superimposed. In Figure 6b, the particles are much smaller, different shapes, and much more evenly distributed, together with plastic particles in the nm range. In fact, when a DSM decomposes into nm range fragments (the

latter are shown by SEM in Figure 6b), it is of particular environmental concern, as the release of nanoplastics is accelerated to due increased surface area.

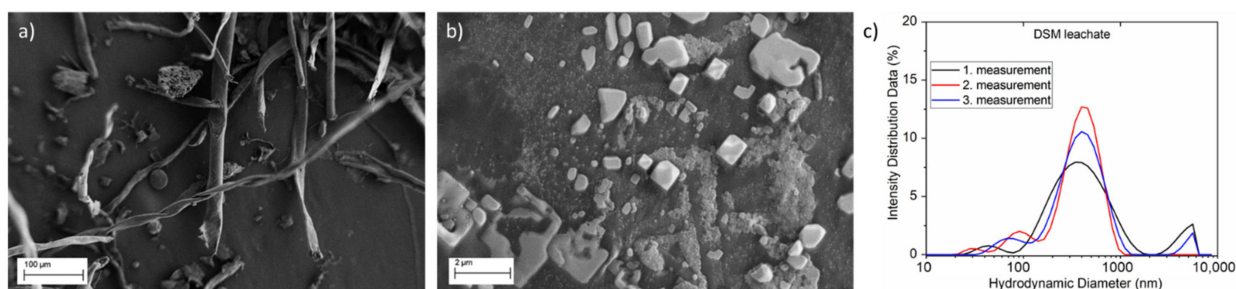


Figure 6. Scans of micro- and nanoparticles released from whole DSM sample in TCLP process. (a) SEM image of particles loaded on the filter, (b) SEM image of filtrate, and (c) particle size distribution of filtrate.

In addition, to prove the leaching of nanoplastic particles in the filtrate of whole DSM leachate, particle size distribution (PSD) analysis, which was recorded three times, was performed (Figure 6c). With this analysis, the presence of nanoscale particles released by DSMs was confirmed. The particles have an average diameter of 305 nm. The majority of the particles (87%) have a diameter of 430 nm, with a standard deviation of 196.1 nm.

3.4. Photodegradability Results by Mimicking Natural Conditions with Xenotest

In general, disposable masks are exposed to the environment after use if not properly stored as waste, which means that the various environmental conditions and their influence should be studied over time. Therefore, in the following section, the DSMs were exposed to environmental conditions using a Xenotest climate chamber. After a long period of mimicking natural conditions (i.e., light, rain, etc., see Section 2.5), the DSMs were evaluated using various characterization techniques after mimicking natural weathering and compared to the untreated DSMs. It is very hard to assess the correlation between artificial weathering and natural weathering in general, as it depends on the type of material. According to Badji et al. [37], artificial weathering in a climate chamber is comparable to a 7.35 times longer period under natural weathering in equatorial regions. Further north and south from the equator, the acceleration time will be above this value. In accordance with Badji et al.'s study, it can be concluded that 200 cycles of artificial weathering, the duration of which was 100 h, are roughly equal to 735 h or 1 month under natural weathering in the equatorial region. Unlike other studies [18], which only investigated the change in properties of disposable masks under UV light weathering conditions, this study implements real daylight, rain, and other environmental parameters typical of real conditions.

The experiments on DSMs using Xenotest revealed that the changes are dramatic after artificial weathering. As is shown in Figure 7a, photodegradation of the three-layered part after 200 repetitions of a 30 min cycle is visually apparent (DSMs decay and become friable). This could be due to changes in chemical composition and fiber structure, which could be seen in the mask fragments broken into smaller pieces. The DSM polymer becomes more fragile, releasing even more microplastics and nanoplastics. In addition, it is suspected that the mechanical strength changed and most likely decreased. The test has shown that the three-layered part of the DSM loses more than 80% of its weight after 200 repetitions under simulated natural conditions in the Xenotest chamber as is shown in Figure 7b. Six samples of the three-layered part were analyzed (B–G) and, as can be seen from the graph of mass loss, the results of photodegradation are satisfyingly precise and show repeatability. This is also the part of the mask that degrades faster than other parts (Figure 7), as weight change in ear loops after 150 repetitions was 3.37% and after 200 repetitions it was 11.14%, and that of nose wires after 150 repetitions was 0.31% and after 200 repetitions it was 0.97%. These results show a significant influence of photodegradation of the masks, contributing to an

increased number of micro/nanoplastics fragments in terms of weight change, confirmed by the DLS analysis below. Aged mask fragments have already been shown to completely transform into microplastics and it was predicted that a fully aged mask would release billions of microplastic fibers into the environment [17]. However, the contribution of more problematic nanoplastics has not been considered.

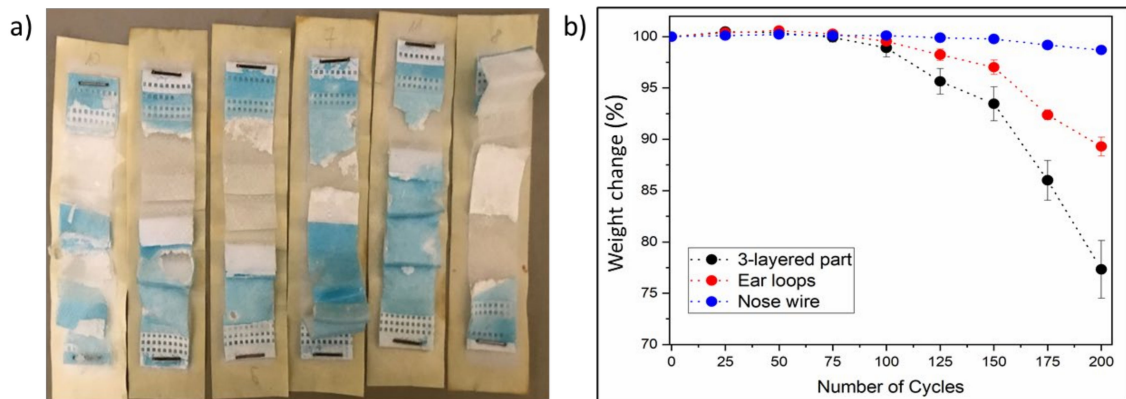


Figure 7. (a) Photodegradation analysis of DSM: (b) mass loss of DSM parts exposed to artificial weathering from 0 to 200 cycles.

FTIR analyses were performed before and after the Xenotest. The FTIR spectra changed only in the case of the three-layered part. In the case of the nose wire and ear loops, there were no visible changes in the collected spectra. Similar to the spectra collected from microplastics after the TCLP are the spectra of photodegraded DSMs (Figure 8). The FTIR spectrum of the photodegraded three-layered part does not agree with the spectrum of polypropylene and shows new peaks around 3300 cm^{-1} , 1730 cm^{-1} , and 1650 cm^{-1} and peaks in the range of $1030\text{--}1060\text{ cm}^{-1}$. Listed signals at corresponding wavenumbers are typical for O-H, C=O, C-O, etc. vibrations [16,18]. The latter indicates that polypropylene undergoes oxidation/degradation reactions, as already observed above in Figure 4.

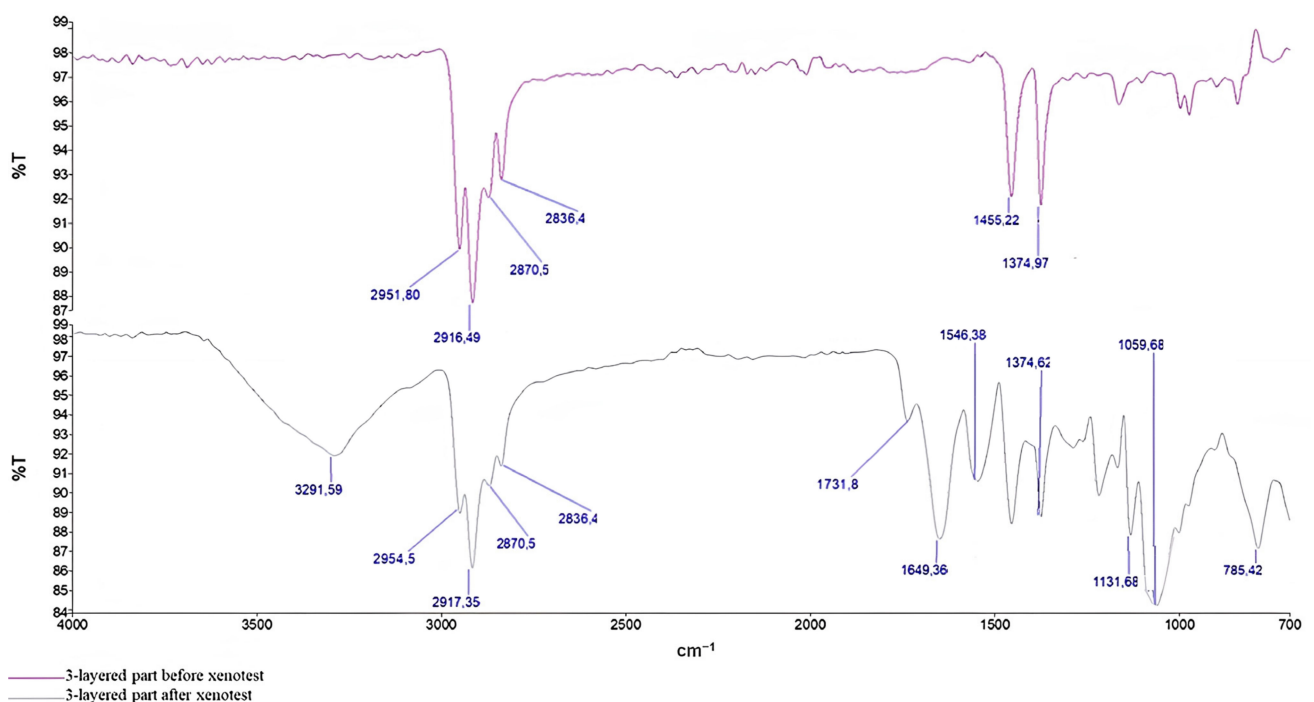


Figure 8. FTIR spectra of the 3-layered part before and after Xenotest.

The changes can also be seen in the TGA and DSC diagrams of the three-layer part of DSMs. The diagrams in Figure 9a,b show that 97% of the mass loss starts at lower temperatures—between 90 °C and 600 °C. The total mass loss from onset to 694.7 °C is 98.8%, in agreement with waste analysis (Table 2). Yet, after mimicking the real natural conditions in Xenotest, the three-layer part of DSMs after exposure seems less thermogravimetrically stable in comparison to virgin three-layer parts, as it loses its mass at a lower T than pristine three-layer parts. In addition, the approximate melting temperature of the DSM after the Xenotest is also lower—156 °C—as can be seen in Figure 9b. The phase transition flow T value for PP was determined to be around 160 °C [7], which coincides with our data and confirms that DSMs are mainly fabricated using PP polymer.

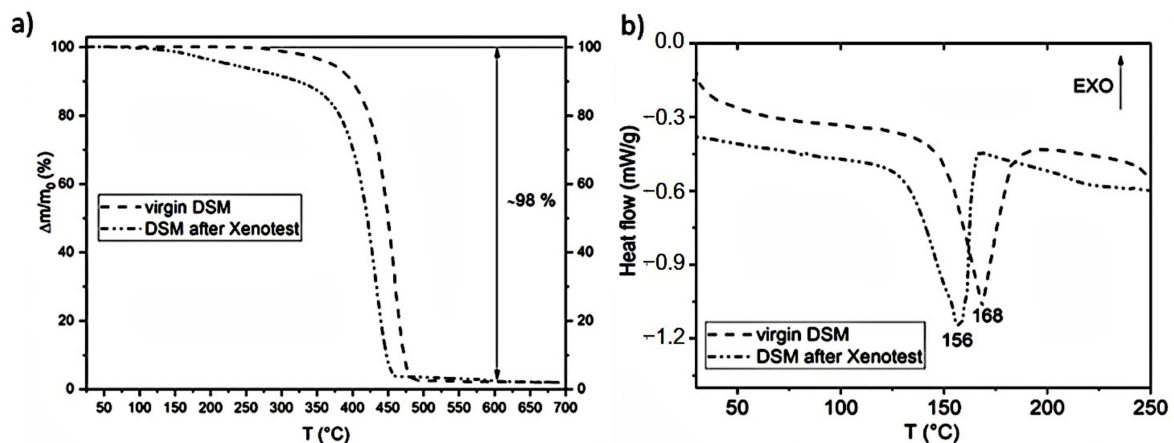


Figure 9. TGA (a) and DSC (b) analyses of whole DSM before and after Xenotest.

The simulated rainwater was collected during the test and analyzed under the optical microscope, which allowed us to isolate microplastic particles produced by photodegradation. As can be seen in Figure 10a, a DSM is degraded by photodegradation into extremely inhomogeneous microparticles, ranging from a few hundred micrometers to less than 1 μm . The formation of nanoplastics and their presence in the simulated rainwater were additionally confirmed by DLS analysis, the result of which can be seen in Figure 10b.

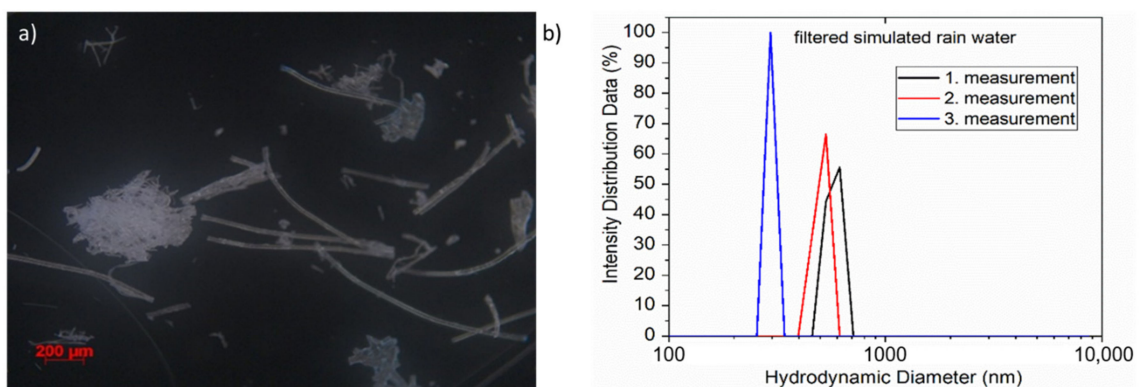


Figure 10. (a) Obtained microplastic parts from collected simulated rainwater; (b) DLS analysis of filtered simulated rainwater.

4. Discussion and Proposed Future Recommendations

To conclude, when we talk about DSM waste, we are talking about the waste that has been with us for a long time, but since the beginning of the epidemic, the quantities have increased dramatically. Given the volumes that are being generated, it is important to understand the wastes that we are dealing with. As we pointed out in the study, it is a homogeneous type of waste—each mask is made up of only five components and is

primarily made of polypropylene. However, this should not lead us to forget about the awareness of the hazardous nature of the waste. As can be seen, this waste contains quite a high amount of Cl, which may indicate the presence of halogenated organic compounds (AOX). However, the main problem is the amount of microplastics and nanoplastics detected in this study, which are formed in a short time when this waste is exposed to natural conditions such as leaching, moisture, temperature, and UV radiation. Thus, it is highly recommended that these strategies are taken into consideration:

- Rapid fragmentation in the environment is an additional problem if this type of waste is not properly collected and processed. Given these considerations, proper disposal of DSM waste should be a priority for the system and the public [38]. In this way, the risks posed by the disposed masks could be better assessed and they could be prevented from entering the environment. Stricter management of mask waste would be beneficial, greatly limiting the amount of masks released into the environment. Such a setting would thus contribute to the control of micro/nanoplastics in the environment.
- A promising option that can open a new way to reduce the released fragments of micro/nanoplastics is recycling. Effective recycling could be another waste management option that would add value along with possible upgrades using various antiviral (nano)fillers. Another promising option would be to reuse the masks to minimize contamination. Reuse could be ensured by disinfection, but special care should be taken here to avoid damaging the fiber structures in the mask or reducing their efficiency in terms of protection or breathability.
- Additional research is needed to determine the best possible way to dispose of DSM waste, whether through energy or material recovery.
- Of particular importance would be bio-based and potentially biodegradable alternatives to current conventional plastic masks. Bio-based materials, including biopolymers, could partially or even completely replace petroleum-based polymers and in this way reduce the ecological footprint.
- Last, but not least, more consideration should be given to ecotoxicological measures. The need to assess the risk of released micro/nanoplastics in the environment should be investigated.

Author Contributions: A.E.: Formal analysis, Investigation, Methodology, Analysis, Visualization, Writing—original draft. O.P.: Analysis, Visualization, Data curation, Writing—review and editing. L.F.Z.: Funding acquisition, Supervision, Methodology, Writing—review and editing. J.V.V.: Conceptualization, Methodology, Funding acquisition, Formal analysis, Supervision, Writing—review and editing. All authors have read and agreed to the published version of the manuscript.

Funding: The authors would like to acknowledge the financial support provided by the Slovenian Research Agency (Grant Number: P2-0118 within COVID Programme and Young Researchers Programme and project No. J7-3149).

Institutional Review Board Statement: Not applicable.

Informed Consent Statement: Not applicable.

Data Availability Statement: Data available on request.

Conflicts of Interest: The authors declare that they have no known competing financial interest or personal relationships that could have appeared to influence the work reported in this paper.

References

1. Shashoua, Y. *Conservation of Plastics*; Taylor & Francis: London, UK, 2008. [[CrossRef](#)]
2. PlasticsEurope. *Plastics—the Facts 2019*; PlasticsEurop: Brussels, Belgium, 2019.
3. World Health Organization. *WHO Director-General's Opening Remarks at the Media Briefing on COVID-19-3 March 2020*; World Health Organization: Geneva, Switzerland, 2020.

4. Park, C.-Y.; Kim, K.; Roth, S.; Beck, S.; Kang, J.W.; Tayag, M.C.; Griffin, M. *Global Shortage of Personal Protective Equipment amid COVID-19: Supply Chains, Bottlenecks, and Policy Implications*; Asian Development Bank: Mandaluyong, Philippines, 2020. [[CrossRef](#)]
5. Czigany, T.; Ronkay, F. The coronavirus and plastics. *Express Polym. Lett.* **2020**, *14*, 510–511. [[CrossRef](#)]
6. Rathinamoorthy, R.; Balasaraswathi, S.R. Disposable tri-layer masks and microfiber pollution—An experimental analysis on dry and wet state emission. *Sci. Total Environ.* **2022**, *816*, 151562. [[CrossRef](#)] [[PubMed](#)]
7. Aragaw, T.A. Surgical face masks as a potential source for microplastic pollution in the COVID-19 scenario. *Mar. Pollut. Bull.* **2020**, *159*, 111517. [[CrossRef](#)] [[PubMed](#)]
8. Sun, J.; Yang, S.; Zhou, G.; Zhang, K.; Lu, Y.; Jin, Q.; Lam, P.; Leung, K.; He, Y. Release of microplastics from discarded surgical masks and their adverse impacts on the marine copepod *Tigriopus japonicus*. *Environ. Sci. Technol. Lett.* **2021**, *8*, 1065–1070. [[CrossRef](#)]
9. Spennemann, D.H.R. COVID-19 Face Masks as a Long-Term Source of Microplastics in Recycled Urban Green Waste. *Sustainability* **2022**, *14*, 207. [[CrossRef](#)]
10. Akber Abbasi, S.; Khalil, A.B.; Arslan, M. Extensive use of face masks during COVID-19 pandemic: (micro-)plastic pollution and potential health concerns in the Arabian Peninsula. *Saudi J. Biol. Sci.* **2020**, *27*, 3181–3186. [[CrossRef](#)] [[PubMed](#)]
11. Akhbarizadeh, R.; Dobaradaran, S.; Nabipour, I.; Tangestani, M.; Abedi, D.; Javanfekr, F.; Jeddi, F.; Zendehtboodi, A. Abandoned Covid-19 personal protective equipment along the Bushehr shores, the Persian Gulf: An emerging source of secondary microplastics in coastlines. *Mar. Pollut. Bull.* **2021**, *168*, 112386. [[CrossRef](#)] [[PubMed](#)]
12. Allison, A.; Ambrose-Dempster, E.; Domenech, T.; Bawn, M.; Arredondo, M.; Chau, C.; Chandler, K.; Dobrijevic, D.; Hailes, H.; Lettieri, P.; et al. The environmental dangers of employing single-use face masks as part of a COVID-19 exit strategy. In *UCL Open: Environment Preprint*; UCL Press: London, UK, 2020. [[CrossRef](#)]
13. Ammendolia, J.; Saturno, J.; Brooks, A.L.; Jacobs, S.; Jambeck, J.R. An emerging source of plastic pollution: Environmental presence of plastic personal protective equipment (PPE) debris related to COVID-19 in a metropolitan city. *Environ. Pollut.* **2021**, *269*, 116160. [[CrossRef](#)] [[PubMed](#)]
14. Parashar, N.; Hait, S. Plastics in the time of COVID-19 pandemic: Protector or polluter? *Sci. Total Environ.* **2021**, *759*, 144274. [[CrossRef](#)] [[PubMed](#)]
15. Patrício Silva, A.L.; Prata, J.C.; Mouneyrac, C.; Barcelò, D.; Duarte, A.C.; Rocha-Santos, T. Risks of Covid-19 face masks to wildlife: Present and future research needs. *Sci. Total Environ.* **2021**, *792*, 148505. [[CrossRef](#)] [[PubMed](#)]
16. Saliu, F.; Veronelli, M.; Raguso, C.; Barana, D.; Galli, P.; Lasagni, M. The release process of microfibers: From surgical face masks into the marine environment. *Environ. Adv.* **2021**, *4*, 100042. [[CrossRef](#)]
17. Shen, M.; Zeng, Z.; Song, B.; Yi, H.; Hu, T.; Zhang, Y.; Zeng, G.; Xiao, R. Neglected microplastics pollution in global COVID-19: Disposable surgical masks. *Sci. Total Environ.* **2021**, *790*, 148130. [[CrossRef](#)] [[PubMed](#)]
18. Wang, Z.; An, C.; Chen, X.; Lee, K.; Zhang, B.; Feng, Q. Disposable masks release microplastics to the aqueous environment with exacerbation by natural weathering. *J. Hazard. Mater.* **2021**, *417*, 126036. [[CrossRef](#)] [[PubMed](#)]
19. Morgana, S.; Casentini, B.; Amalfitano, S. Uncovering the release of micro/nanoplastics from disposable face masks at times of COVID-19. *J. Hazard. Mater.* **2021**, *419*, 126507. [[CrossRef](#)] [[PubMed](#)]
20. *SIST-TP CEN/TR 15310-4:2007*; Characterization of Waste—Sampling of Waste Materials—Part 4: Guidance on Procedures for Sample Packaging, Storage, Preservation, Transport and Delivery. SIST: Newark, DE, USA, 2007.
21. Government of the Republic of Slovenia. *Rules on the Characterisation of Waste Prior to Landfill, the Characterisation of Hazardous Waste Prior to Incineration and the Performance of Chemical Analysis of Waste for Control Purposes*; 2016-01-2488; Government of the Republic of Slovenia: Ljubljana, Slovenia, 2016.
22. *SIST EN 15002:2015*; Characterization of Waste—Preparation of Test Portions from the Laboratory Sample. SIST: Newark, DE, USA, 2015.
23. *SIST EN 15411:2011*; Solid Recovered Fuels—Methods for the Determination of the Content of Trace Elements (As, Ba, Be, Cd, Co, Cr, Cu, Hg, Mo, Mn, Ni, Pb, Sb, Se, Tl, V and Zn). SIST: Newark, DE, USA, 2011.
24. *SIST EN 13137:2002*; Characterization of Waste—Determination of Total Organic Carbon (TOC) in Waste, Sludges and Sediments. SIST: Newark, DE, USA, 2002.
25. *SIST EN 16168:2013*; Sludge, Treated Biowaste and Soil—Determination of Total Nitrogen Using Dry Combustion Method. SIST: Newark, DE, USA, 2013.
26. Ebeling, M.E. The Dumas Method for Nitrogen in Feeds. *J. Assoc. Off. Anal. Chem.* **2020**, *51*, 766–770. [[CrossRef](#)]
27. *SIST EN 15935:2012*; Sludge, Treated Biowaste, Soil and Waste—Determination of Loss on Ignition. SIST: Newark, DE, USA, 2012.
28. *SIST EN 15934:2012*; Sludge, Treated Biowaste, Soil and Waste—Calculation of Dry Matter Fraction after Determination of Dry Residue or Water Content. SIST: Newark, DE, USA, 2012.
29. *SIST-TS CEN/TS 16023:2014*; Characterization of Waste—Determination of Gross Calorific Value and Calculation of Net Calorific Value. SIST: Newark, DE, USA, 2014.
30. *SIST EN 15308:2017*; Characterization of Waste—Determination of Selected Polychlorinated Biphenyls (PCB) in Solid Waste by Gas Chromatography with Electron Capture or Mass Spectrometric Detection. SIST: Newark, DE, USA, 2017.
31. *SIST EN 14582:2017*; Characterization of Waste—Halogen and Sulfur Content—Oxygen Combustion in Closed Systems and Determination Methods. SIST: Newark, DE, USA, 2017.
32. Method 1311 Toxicity Characteristic Leaching Procedure. EPA: Washington, DC, USA, 1992.

33. Potrč, S.; Kraševac Glaser, T.; Vesel, A.; Poklar Ulrih, N.; Fras Zemljič, L. Two-Layer Functional Coatings of Chitosan Particles with Embedded Catechin and Pomegranate Extracts for Potential Active Packaging. *Polymers (Basel)* **2020**, *12*, 1855. [[CrossRef](#)] [[PubMed](#)]
34. Glaser, T.K.; Plohl, O.; Vesel, A.; Ajdnik, U.; Ulrih, N.P.; Hrnčič, M.K.; Bren, U.; Fras Zemljič, L. Functionalization of Polyethylene (PE) and Polypropylene (PP) Material Using Chitosan Nanoparticles with Incorporated Resveratrol as Potential Active Packaging. *Materials* **2019**, *12*, 2118. [[CrossRef](#)] [[PubMed](#)]
35. Porubská, M.; Szöllös, O.; Kóňová, A.; Janigová, I.; Jašková, M.; Jomová, K.; Chodák, I. FTIR spectroscopy study of polyamide-6 irradiated by electron and proton beams. *Polym. Degrad. Stab.* **2012**, *97*, 523–531. [[CrossRef](#)]
36. Dincer, I.; Rosen, M.A.; Khalid, F. 3.16 Thermal Energy Production. In *Comprehensive Energy Systems*; Dincer, I., Ed.; Elsevier: Oxford, UK, 2018; pp. 673–706. [[CrossRef](#)]
37. Badji, C.; Soccalingame, L.; Garay, H.; Bergeret, A.; Bénézet, J.-C. Influence of weathering on visual and surface aspect of wood plastic composites: Correlation approach with mechanical properties and microstructure. *Polym. Degrad. Stab.* **2017**, *137*, 162–172. [[CrossRef](#)]
38. Remic, K.; Erjavec, A.; Volmajer Valh, J.; Šterman, S. Public Handling of Protective Masks from Use to Disposal and Recycling Options to New Products. *J. Mech. Eng.* **2022**, *68*, 281–289. [[CrossRef](#)]